Quasi-one-dimensional diffuse laser cooling of atoms

Jin-Yin Wan,[1] Xin Wang,[2] Xiao Zhang,[2] Yan-Ling Meng,[1] Wen-Li Wang,[1] Yuan Sun,[2,*] and Liang Liu[1,†]

[1]*Laboratory of Space Laser Engineering and Technology, Shanghai Institute of Optics and Fine Mechanics, Chinese Academy of Sciences, Shanghai 201800, China*

[2]*Key Laboratory of Quantum Optics and Center of Cold Atom Physics, Shanghai Institute of Optics and Fine Mechanics, Chinese Academy of Sciences, Shanghai 201800, China*

(Received 30 November 2021; accepted 8 March 2022; published 28 March 2022)

We demonstrate experimentally the generation of one-dimensional cold gases of ^{87}Rb atoms by diffuse laser cooling. A horizontal slender vacuum glass tube with a length of 105 cm and diameter of 2 cm is used in our experiment. The diffuse laser light inside the tube, which is generated by multireflection of injected lasers, cools the background vapor atoms. With 250 mW of cooling light and 50 mW of repumping light, an evenly distributed 1-m-long profile of cold atom cloud is obtained. We observe a factor 4 improvement in the atomic optical density for a typical cooling duration of 170 ms and a sub-Doppler atomic temperature of 25 μK. The central number of detected cold atoms remains constant for a free-fall duration of 30 ms. Such samples are ideal for many quantum optical experiments involving electromagnetically induced transparency, electronically highly excited (Rydberg) atoms, and quantum precision measurements.

DOI: 10.1103/PhysRevA.105.033110

I. INTRODUCTION

Laser cooling techniques have revolutionized experimental research on cold-atom physics and become a standard tool for precision measurement, quantum optics, quantum simulation, quantum computation, and quantum information [1]. One typical laser cooling apparatus is the six-beam magneto-optical trap (MOT) requiring careful alignment of the cooling laser beams and magnetic gradient field, which makes the development of precise metrological devices based on cold atoms such as atomic clocks, gravimeters, and gyroscopes difficult and complex. A diffuse laser cooling (DLC) scheme is proposed to ease these problems, where the diffuse light field is generated in a tube or a sphere whose inner surface reflects laser light diffusely [2–5]. Three-dimensional diffuse light cooling configurations have been realized on Cs and Rb vapors in spherical cells [6,7], which present a Sisyphus-like cooling mechanism since the cold atoms can reach a sub-Doppler temperature as low as 3.5 μK [6,8,9]. The DLC technique is easy and robust since it needs no alignment of lasers and is not sensitive to the magnetic field. Diffuse laser cooling has been widely applied to compact microwave atomic clocks for ground operation and onboard applications in a microgravity environment [10–14]. Moreover, the compact cold-atom platform provides exciting possibilities for portable, robust, and accessible quantum sensors. Therefore, a neutral cold-atom ensemble by the DLC technique is also a potential candidate for space applications [15–17].

The DLC technique has been studied both in slowing an atomic beam and in cooling atoms from a vapor background [2–7]. Much effort has been put forth in investigating the properties of cold atoms captured by DLC including temperature, atomic density, localization, scale, and spectroscopic effects [18–25]. However, much less attention has been paid to the one-dimensional configuration. In this work we demonstrate a 1-m-long diffuse laser cooling apparatus in which ^{87}Rb atoms are cooled in a nearly-one-dimensional shape by DLC. Different from the conventional DLC setups [6,7,25], we employ a horizontal slender glass tube whose outside surface is covered by a reflective material. Atoms are cooled homogeneously by diffuse light inside the tube.

The paper is organized as follows. In Sec. II the experimental configuration for the DLC of ^{87}Rb atoms in the horizontal slender glass tube and the corresponding time sequence are presented. In Sec. III, as a key parameter to determine the performance of the captured cold atoms, the dependence of the atomic optical density (OD) on a variety of experimental parameters, including the cooling light power, the repumping light power, the detuning of cooling, and the probe light, are measured. The cooling time and temperature measurement of the cold atoms are also described. The atomic density distributions of the cold atoms in the longitudinal direction are detected through a pair of moving Helmholtz coils. The paper is summarized in Sec. IV.

II. EXPERIMENTAL CONFIGURATION

Figure 1 gives the experimental scheme. Two extended-cavity diode lasers (ECDLs) tuned at 780.24 nm of the rubidium D_2 line are used, both of which are frequency locked by saturation absorption spectra. One is used for both cooling and the probe and the other is used for the repumping, as shown in Fig. 1(a). Each laser frequency is individually controlled by acousto-optic modulators (AOMs).

*sunyuan@siom.ac.cn
†liang.liu@siom.ac.cn

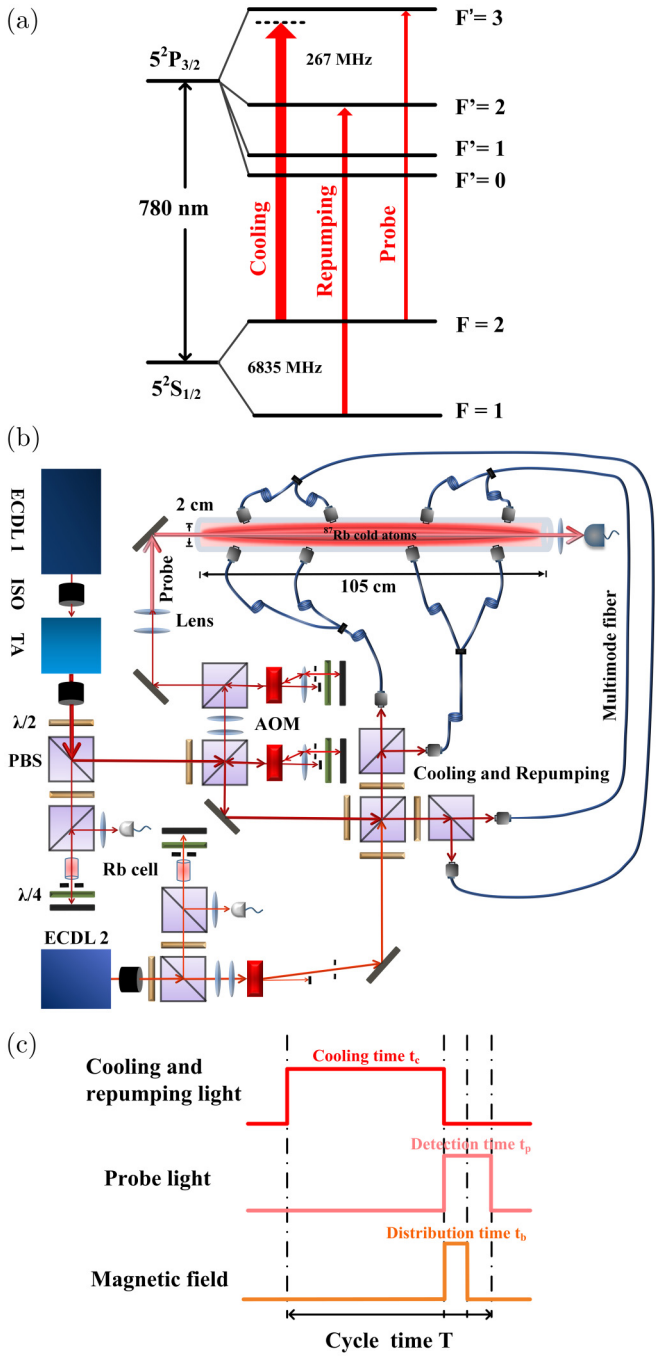

FIG. 1. DLC measurement scheme. (a) Relevant energy levels of the ^{87}Rb D_2 line for diffuse light cooling. (b) Schematic of the experimental setup: ECDL 1, extended-cavity diode laser 1, cooling and probe laser; ECDL 2, repumping laser; TA, tapered amplifier; ISO, isolator; PBS, polarization beam splitter; $\lambda/2$, half waveplate; $\lambda/4$, quarter waveplate; HR, high-reflection mirror; PD, photo detector; and AOM, acoustic optical modulator. (c) DLC and atomic density distribution measurement timing sequence. In our case, the cooling time t_c is 170 ms, the probe time t_p is 100 ms, the distribution magnetic field time t_b is 50 ms, and the cycle time T is 270 ms.

Similar to traditional optical molasses, there are four energy levels of ^{87}Rb atoms involved in our DLC experiment. The cooling light is red detuned by around -17 MHz ($\sim 2.8\Gamma$, where $\Gamma = 6.056$ MHz is the natural linewidth of ^{87}Rb) to the transition $5\,^2S_{1/2}, F = 2 \rightarrow 5\,^2P_{3/2}, F' = 3$. The repumping light is resonant with the transition $5\,^2S_{1/2}, F = 1 \rightarrow 5\,^2P_{3/2}, F' = 2$ to prevent ^{85}Rb atoms from accumulating in the $5\,^2S_{1/2}, F = 1$ energy level. The probe light is nearly resonant with the transition $5\,^2S_{1/2}, F = 2 \rightarrow 5\,^2P_{3/2}, F' = 3$.

A sketch of the experimental setup is shown in Fig. 1(b). The main physical part is a horizontal cylindrical glass vacuum tube with a length of 105 cm and an inner cross section diameter of 2 cm, whose vacuum is maintained at 3×10^{-8} Pa by an ion pump. Its outside surface is covered with a coating whose diffuse reflectance is more than 98% at an optical wavelength of 780 nm. Small holes are scratched for the transmission of light beams. Homogeneous diffuse light inside the tube is formed from diffuse multireflection of lasers which are injected through eight holes. The vacuum tube is filled with natural rubidium vapor which is composed of ^{87}Rb (27.8%) and ^{85}Rb (72.2%). The Rb vapor is obtained by heating the Rb source to 70 °C to release gaseous atoms. The source is then cooled down slowly to room temperature ($\sim$25 °C).

The optical system mainly consists of two ECDLs, both of which are frequency locked by saturated absorption technique. One ECDL is locked at the transition $5\,^2S_{1/2}, F = 2$ to the crossover peak of $5\,^2P_{3/2}, F' = 1$ and $5\,^2P_{3/2}, F' = 3$. It is followed by a tapered amplifier, which can emit a maximum light power of 2 W. The output beam is then divided into two beams via a polarizing beam splitter (PBS). One beam serves as the cooling light and the other beam serves as the probe light. Each beam is switched and frequency shifted from a certain transition by using an AOM in the double-pass configuration. The other ECDL is frequency locked at the transition $5\,^2S_{1/2}, F = 1$ to the crossover peak of $5\,^2P_{3/2}, F' = 1$ and $5\,^2P_{3/2}, F' = 2$. It serves as the repumping light which is controlled by an AOM in the single-pass configuration. First, the cooling beam and repumping beam are combined by a PBS. Second, the two combined beams are divided into four balanced beams by another two PBSs. Third, each beam is coupled into a one-to-two multimode optical fiber and eight intensity-balanced divergent lights are generated. Finally, the fiber coupling heads are injected into the tube from the eight evenly distributed holes on the side surface. The injection angles can be between 30° and 60° from the side section; thus there is no need to optimize the alignment of these beams. Compared with the well-designed optical alignments, this robust optical injection mode reduces the difficulty of the optical adjustment.

Figure 1(c) shows the experimental sequence of the DLC process. The cooling and repumping lights are applied for 170 ms. This process will cool a large population of ^{87}Rb atoms down from the background Rb vapor; the internal state of such ^{87}Rb atoms is prepared in the energy level of $5\,^2S_{1/2}, F = 2$. Then the probe light is applied for 100 ms to detect the captured cold atoms. In the first 50 ms of the probe time, a weak static magnetic field is applied to measure the atomic density distribution. The total cycle time is 270 ms.

III. RESULTS AND DISCUSSION

Atoms cooled by DLC in the tube are detected by measuring absorption of a resonant probe laser in the direction of

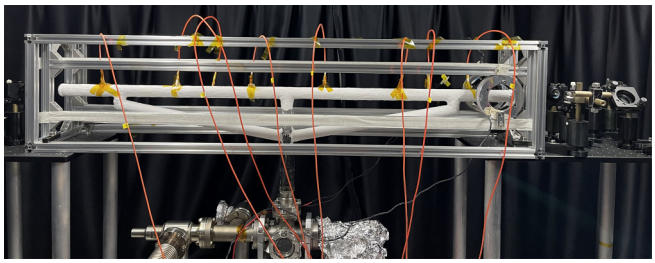

FIG. 2. Photograph of the experimental vacuum system. The main physical part is a horizontal cylindrical glass vacuum tube with a length of 105 cm and an inner cross-section diameter of 2 cm, whose vacuum is maintained at 3×10^{-8} Pa by an ion pump. Its outside surface is covered with a coating whose diffuse reflectance is more than 98% at an optical wavelength of 780 nm. Small holes are scratched for the transmission of light beams.

the tube's axis, as shown in Fig. 1(b). A photograph of the experimental vacuum system and how it is built is shown in Fig. 2. The diameter of the Gaussian probe beam is 1 mm with intensity around 100 μW/cm^2. Generally, the OD of the cold atoms is given by the relation $I = I_0 e^{-\mathrm{OD}}$, where I_0 and I are the incident and the output intensity, respectively. The density of cold atoms n obeys the relation $\mathcal{D} = \sigma nL$, where $\mathcal{D}$ is the optical density, σ is the cross section of the atom-light interaction, and L is the length of cold atoms. The maximum number of cold atoms can be reached at the balance between capture and loss of laser-cooled atoms. A straightforward phenomenological model may be given as $dN/dt = -\kappa N + \alpha$, where N is the number of cold atoms, κ is the loss, and α is the replenishing rate of the newly captured cold atoms [1]. Therefore, $N(t) = (\alpha/\kappa)(1 - e^{-\kappa(t-t_0)})$, and $N(\infty) = \alpha/\kappa$ when t is long enough.

Figure 3(a) shows the normalized cold-atom number versus the cooling time t_c. The fit, shown by the solid line in Fig. 3(a), gives the loss rate κ as 17.6 s^{-1}. The loss mechanism is mainly due to the gravity and the cold-atom expansion. When the cooling time lasts more than 0.17 s, the number of cold atoms reaches saturation, which is about 6 times faster than the previous typical DLC schemes [25]. The fast balance comes from the quick loss of cooled atoms due to the small diameter of the tube, which is horizontally placed in gravity.

In order to determine the temperature of the captured cold atoms, we use a recently developed nearly nondestructive thermometry of labeled cold atoms. In this work we approximate all the detected atoms after the cooling process to be at the energy level of $5\,^2S_{1/2}, F = 2$, neglecting the polarization degree of freedom. The number of cold atoms within the beam size of the probe light will decrease over the probe time caused by spatial expansion and gravity. The effect of gravity is neglected for simplicity since the expansion time of the labeled atoms is rather short. The temperature of the cold-atom ensemble can be evaluated by the detection of the probe light over time. Moreover, the dynamics along the axis of the slender cavity rarely affects the signal. Therefore, the process can be considered in a two-dimensional (2D) setting in the transverse plane. In addition, the speed distribution of the cold atoms is well described by the 2D Maxwell-Boltzmann distribution $f(v)dv = (\frac{m}{2\pi\kappa_B T})2\pi v \exp(-\frac{mv^2}{2\kappa_B T})dv$

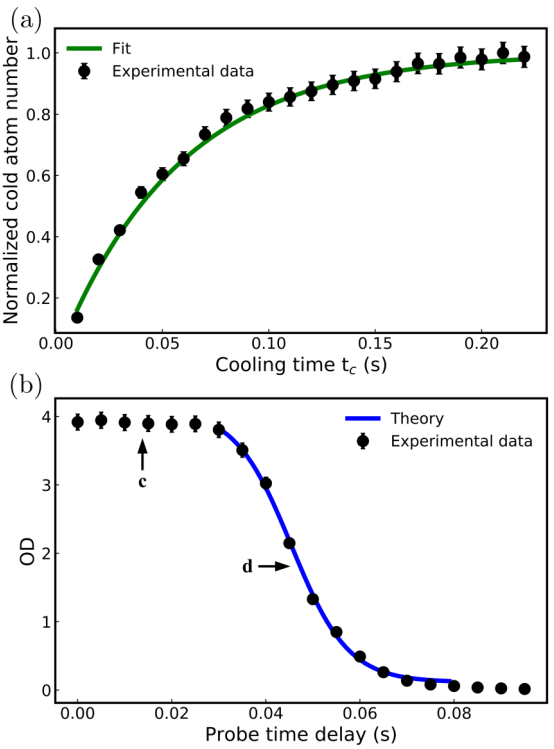

FIG. 3. (a) Normalized cold-atom number along the optical detection axis versus the cooling time t_c, where the atom number has been normalized to a factor of 8×10^9. For a cooling time longer than about 0.17 s, saturation behavior occurs where the capture and loss are almost balanced. (b) Measured OD at different probe time delays. A significant result of the maximum OD remains unchanged for a free-fall duration of 30 ms, as indicated by the arrow labeled c. Here the density of cold atoms is on the order of 10^7 cm^{-3}. Arrow d indicates that it decreases exponentially with a theoretical fitting, where a temperature of 25 μK is obtained.

and the cold-atom number detected in the range of the probe beam with radius r is proportional to [25]

$$s(r,t) = 1 - \exp\left(-\frac{m(r/t)^2}{2k_B T}\right). \tag{1}$$

The experimental results and fitting are shown in Fig. 3(b). The arrow labeled c indicates that the measured OD almost stays at the maximum for the free-fall duration of 30 ms, since the density distribution of the targeted cold atoms on the optical detection axis remains unchanged. It is the first observation of a nearly fixed maximum cold-atom number in the detection region in a time range of tens of milliseconds once the cooling light is switched off. The constancy is partly due to the small diameter of the probe beam relative to the cross section. Generally, the number of captured cold atoms starts to decrease immediately when there is no cooling light [7], which would be limited by the gravity and thermal expansion of the cloud. Arrow d indicates the thermal expansion process of the addressed atoms with the theoretical fitting curve according to Eq. (1), where the temperature is deduced to be 25 μK. This demonstrates that a sub-Doppler coolinglike mechanism exists which is caused by the disordered gradient forces formed in the diffuse light field.

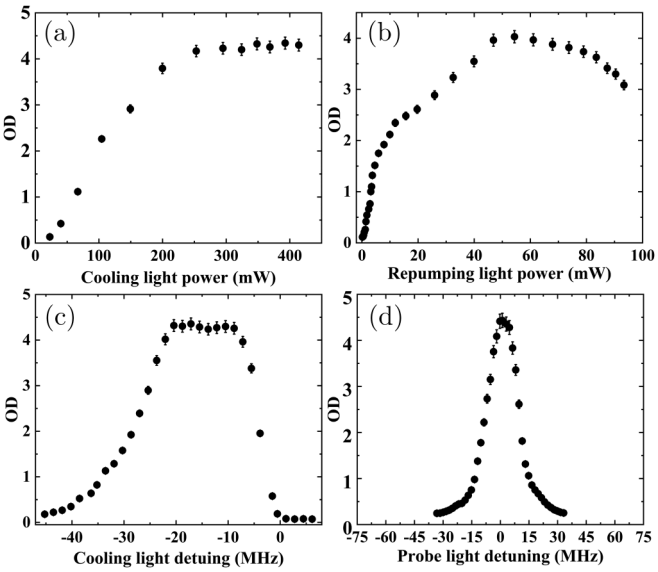

FIG. 4. Measured OD as a function of various cooling parameters. (a) Plot of OD versus cooling light power when the cooling light is red detuned at 12 MHz and the repumping light power is fixed at 50 mW. (b) Plot of OD versus repumping light power when the cooling light is red detuned at 12 MHz and the cooling light power is fixed at 250 mW. (c) Plot of OD versus cooling light detuning when the cooling light power is 250 mW and the repumping light power is fixed at 50 mW. (d) Plot of OD versus probe light detuning when the cooling light is red detuned at 17 MHz, the cooling light power is 250 mW, and the repumping light power is fixed at 50 mW.

We measured the OD vs the total power of lasers injected into the vacuum tube with a fixed detuning of -12 MHz, a cooling time t_c of 0.17 s, a probe time of 0.1 s, and the repumping power at 50 mW. As shown in Fig. 4(a), the OD increases linearly with the cooling light power and reaches a saturation value when the cooling light power is more than 250 mW.

We set the cooling light power at 250 mW and vary the repumping light power. Figure 4(b) indicates that the OD increases with the repumping light power in the lower power region and reaches saturation at a value of 50 mW. However, a slight decrease is monitored in the higher power region, which is caused by the heating effect of the resonant repumping light. The larger the repumping light power, the greater the heating effect, as shown in Fig. 4(b). As a result, we obtain an atomic OD greater than 4 with a cooling light power of only 250 mW; such a low laser power reduces the complexity of the laser system.

Figure 4(c) shows the measured OD as a function of cooling laser detuning. The measured OD almost maintains a maximum value of 4.3 for the detuning ranging between -20 and -8.8 MHz (about -3.3Γ to -1.4Γ). Different from a MOT or optical molasses, the velocity capture range of DLC is $|\Delta| \leqslant kv \leqslant 2|\Delta|$ [2], where Δ denotes the detuning of the cooling light, k is the wave vector, and v is the atomic velocity. Such a wide capture range allows capturing atoms with a large range of velocities.

We measured the atomic OD versus the probe light detuning as shown in Fig. 4(d). It shows a Lorentzian curve with the full width at half maximum much larger than the natural linewidth of the transition, which is mainly due to the Doppler effect. The measured OD reaches the largest value of 4.4 when the probe light is resonant with the atomic transition, and therefore all measurements keep the probe light resonant for the estimation of the number of cold atoms.

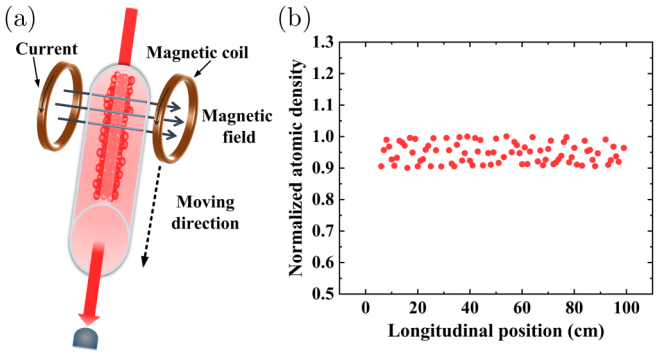

FIG. 5. Atomic density measurement scheme. (a) Atomic density measurement setup. A pair of Helmholtz coils is used to measure the longitudinal atomic density distribution. (b) Measured atomic density distribution along the longitudinal direction of the cavity.

To measure the atomic density distribution in the probe direction, we apply a weak uniform static magnetic field ($\sim$2.3 mT) perpendicular to the tube's longitudinal axis as shown in Fig. 5(a). The magnetic field is generated by a pair of Helmholtz coils with a radius of 5 cm and is distributed on both sides of the tube perpendicularly and equidistantly. Generally, the resonant probe light measures the atoms at the $5\,^2S_{1/2}, F = 2$ energy level. When the atoms' energy level is shifted from resonance by 30 MHz through a static magnetic field as shown in Fig. 4(d), the cold atoms in the magnetic-field region would not be detected by the probe light. The data of these cold atoms can be directly obtained when they are subtracted from the total signal detected without magnetic field. Therefore, we measured the cold-atom density distribution by moving the Helmholtz coils from one end of the tube to the other. In the first 30 ms after the cooling light is switched off, the atomic distribution signal is too small to detect precisely since the cold-atom number is at the maximum and stable in this time region as shown in Fig. 3(b). Thus the atomic density distribution is measured at a probe time delay of 40 ms as shown in Fig. 5(b). The cold-atom number distribution lies in a horizontal line along the longitudinal direction of the tube; thus a 1-m-long nearly-one-dimensional cold-atom cloud is prepared. Since the tube is slender, the light emitted by the multimode optical fibers travels a very short distance before touching the wall and then is diffusely reflected immediately at a high rate. The isotropic light in the horizontal chamber forms a quasi-one-dimensional region which is more evenly distributed than that in the spherical or vertical configurations [21] and it homogenizes the atomic density.

IV. CONCLUSION

We have experimentally demonstrated a nearly-one-dimensional cold ^{87}Rb atom cloud with a length of 105 cm

and a diameter of 2 cm by DLC in a horizontally placed slender glass tube. We have systematically studied the dependence of an atomic OD on several control parameters. With a total cooling power of 250 mW, a repumping power of 50 mW, and a cooling time of 0.17 s, we obtain a horizontal uniformly distributed cold-^{87}Rb-atom ensemble with an atomic OD of more than 4 and a temperature of about 25 μK. We observe that the maximum atomic OD remains almost unchanged for a free-fall duration of 30 ms.

We have also shown the simplicity and robustness of the DLC. In fact, the DLC depends only on the interaction between diffuse light and vapor atoms, regardless of scale, shape, polarization, propagation direction of laser field, etc. Such characteristics make it easy for the DLC to construct a different geometry of the cold-atom cloud [22], which is not possible by MOT or optical molasses; for example, the cold-atom cloud in the 1-m-long tube in this work can be easily extended to a 1-km-long or even longer tube and also to a 2D shape.

Our results provide a method to generate cold atoms especially in some geometries which are useful in quantum sensing.

ACKNOWLEDGMENTS

We thank Weibin Li for helpful suggestions in the preparation of the manuscript. This work was supported by the National Natural Science Foundation of China (Grants No. 92165107 and No. 61727821).

[1] H. J. Metcalf and P. van der Straten, *Laser Cooling and Trapping* (Springer, New York, 1999).

[2] W. Ketterle, A. Martin, M. A. Joffe, and D. E. Pritchard, Slowing and Cooling Atoms in Isotropic Laser Light, Phys. Rev. Lett. **69**, 2483 (1992).

[3] H.-X. Chen, W.-Q. Cai, L. Liu, W. Shu, F.-S. Li, and Y.-Z. Wang, Laser cooling and deceleration of neutral atoms by red-shifted diffuse light, Chin. Phys. Lett. **11**, 541 (1994).

[4] Y.-Z. Wang and L. Liu, Laser manipulation of atoms and atom optics, Aust. J. Phys. **48**, 267 (1995).

[5] H. Batelaan, S. Padua, D. H. Yang, C. Xie, R. Gupta, and H. Metcalf, Slowing of ^{85}Rb atoms with isotropic light, Phys. Rev. A **49**, 2780 (1994).

[6] E. Guillot, P.-E. Pottie, and N. Dimarcq, Three-dimensional cooling of cesium atoms in a reflecting copper cylinder, Opt. Lett. **26**, 1639 (2001).

[7] H.-D. Cheng, W.-Z. Zhang, H.-Y. Ma, L. Liu, and Y.-Z. Wang, Laser cooling of rubidium atoms from background vapor in diffuse light, Phys. Rev. A **79**, 023407 (2009).

[8] P. Horak, J.-Y. Courtois, and G. Grynberg, Atom cooling and trapping by disorder, Phys. Rev. A **58**, 3953 (1998).

[9] G. Grynberg, P. Horak, and C. Mennerat-Robilliard, Spatial diffusion of atoms cooled in a speckle field, Europhys. Lett. **49**, 424 (2000).

[10] F.-X. Esnault, D. Holleville, N. Rossetto, S. Guerandel, and N. Dimarcq, High-stability compact atomic clock based on isotropic laser cooling, Phys. Rev. A **82**, 033436 (2010).

[11] B.-C. Zheng, H.-D. Cheng, Y.-L. Meng, L. Xiao, J.-Y. Wan, and L. Liu, Development of an integrating sphere cold atom clock, Chin. Phys. Lett. **30**, 123701 (2013).

[12] P. Liu, Y.-L. Meng, J.-Y. Wan, X.-M. Wang, Y.-N. Wang, L. Xiao, H.-D. Cheng, and L. Liu, Scheme for a compact cold-atom clock based on diffuse laser cooling in a cylindrical cavity, Phys. Rev. A **92**, 062101 (2015).

[13] M. Langlois, L. De Sarlo, D. Holleville, N. Dimarcq, J.-F. Schaff, and S. Bernon, Compact Cold-Atom Clock for On-board Timebase: Tests in Reduced Gravity, Phys. Rev. Appl. **10**, 064007 (2018).

[14] Y.-N. Wang, Y.-L. Meng, J.-Y. Wan, M.-Y. Yu, X. Wang, L. Xiao, H.-D. Cheng, and L. Liu, Optical-plus-microwave pumping in a magnetically insensitive state of cold atoms, Phys. Rev. A **97**, 023421 (2018).

[15] T. van Zoest, N. Gaaloul, Y. Singh, H. Ahlers, W. Herr, S. Seidel, W. Ertmer, E. Rasel, M. Eckart, E. Kajari *et al.*, Bose-Einstein condensation in microgravity, Science **328**, 1540 (2010).

[16] L. Liu, D.-S. Lü, W.-B. Chen, T. Li, Q.-Z. Qu, B. Wang, L. Li, W. Ren, Z.-R. Dong, J.-B. Zhao *et al.*, In-orbit operation of an atomic clock based on laser-cooled ^{87}Rb atoms, Nat. Commun. **9**, 2760 (2018).

[17] D. C. Aveline, J. R. Williams, E. R. Elliott, C. Dutenhoffer, J. R. Kellogg, J. M. Kohel, N. E. Lay, K. Oudrhiri, R. F. Shotwell, N. Yu, and R. J. Thompson, Observation of Bose-Einstein condensates in an Earth-orbiting research lab, Nature (London) **582**, 193 (2020).

[18] W.-Z. Zhang, H.-D. Cheng, L. Liu, and Y.-Z. Wang, Observation of recoil-induced resonances and electromagnetically induced absorption of diffuse light by cold atoms, Phys. Rev. A **79**, 053804 (2009).

[19] W.-Z. Zhang, H.-D. Cheng, L. Xiao, L. Liu, and Y.-Z. Wang, Nonlinear spectroscopy of cold atoms in diffuse laser light, Opt. Express **17**, 2892 (2009).

[20] X.-C. Wang, H.-D. Cheng, L. Xiao, B.-C. Zheng, Y.-L. Meng, L. Liu, and Y.-Z. Wang, Measurement of spatial distribution of cold atoms in an integrating sphere, Chin. Phys. Lett. **29**, 023701 (2012).

[21] Y.-L. Meng, H.-D. Cheng, P. Liu, B.-C. Zheng, L. Xiao, J.-Y. Wan, X.-M. Wang, and L. Liu, Increasing the cold atom density in an integrating spherical cavity, Phys. Lett. A **378**, 2034 (2014).

[22] B.-C. Zheng, H.-D. Cheng, Y.-L. Meng, P. Liu, X.-M. Wang, L. Xiao, J.-Y. Wan, and L. Liu, A large-scale cold atom source in an integrating sphere, Mod. Phys. Lett. B **28**, 1450116 (2014).

[23] J.-Y. Wan, H.-D. Cheng, Y.-L. Meng, L. Xiao, P. Liu, X.-M. Wang, Y.-N. Wang, and L. Liu, Non-resonant magneto-optical effects in cold atoms, Chin. Opt. Lett. **13**, 020201 (2015).

[24] W.-L. Wang, J.-L. Deng, and Y.-Z. Wang, Recoil-induced resonance spectroscopy and nondestructive temperature measurement of cold rubidium atoms inside an integrating sphere, J. Opt. Soc. Am. B **32**, 2441 (2015).

[25] X. Wang, Y. Sun, H.-D. Cheng, J.-Y. Wan, Y.-L. Meng, L. Xiao, and L. Liu, Nearly Nondestructive Thermometry of Labeled Cold Atoms and Application to Isotropic Laser Cooling, Phys. Rev. Appl. **14**, 024030 (2020).